The Journal of Antibiotics (2019) 72:629–633
https://doi.org/10.1038/s41429-019-0187-7

JARA Japan Antibiotics Research Association
The Society for Actinomycetes Japan

BRIEF COMMUNICATION

New preaustinoids from a marine-derived fungal strain *Penicillium* sp. SF-5497 and their inhibitory effects against PTP1B activity

Jin-Soo Park[1] · Tran Hong Quang[2] · Nguyen Thi Thanh Ngan[3] · Jae Hak Sohn[4] · Hyuncheol Oh[1]

Received: 12 February 2019 / Revised: 22 March 2019 / Accepted: 4 April 2019 / Published online: 24 April 2019

Abstract

Chemical investigation of the marine-derived fungal isolate *Penicillium* sp. SF-5497 resulted in the isolation of two new preaustinoid-related meroterpenoids, named preaustinoid A6 (**1**) and preaustinoid A7 (**2**), along with three known metabolites (**3–5**). Their structures were elucidated by extensive spectroscopic analyses, such as 1D and 2D NMR and MS data. Among these, compounds **1** and **3** inhibited PTP1B activity in a dose-dependent manner, with IC_{50} values of 17.6 and 58.4 μM, respectively. Furthermore, kinetic analyses indicated that compound **1** inhibited PTP1B in a noncompetitive manner, with the K_i value of 17.0 μM.

Marine-derived fungi are considered as rich sources of various classes of bioactive secondary metabolites, of which meroterpenoids are shown to have unique structures with a wide range of chemical diversity. Meroterpenoids that formed via a mixed terpenoid–polyketide biosynthetic pathway were found in many fungal species and marine organisms [1]. In the course of our ongoing searching for the bioactive secondary metabolites from marine-derived fungal isolates [2], we recently reported the isolation of two new meroterpenoids named furanoaustinol and 7-acetoxydehydroaustinol from the extracts obtained from cultures of a marine-derived isolate of *Penicillium* sp. SF-5497 [3]. In our continuing efforts to explore the chemistry of this isolate, five meroterpenoids including two new preaustinoid-related meroterpenoids were encountered, and this study describes the isolation, structural elucidation, and PTP1B inhibitory effects of these metabolites from the EtOAc extract of *Penicillium* sp. SF-5497.

PTP1B, a member of the protein tyrosine phosphatase (PTP) superfamily, is considered as a critical regulator of multiple signaling networks involved in human disorders, such as diabetes, obesity, and cancer [4]. Biochemical, genetic, and pharmacological studies have indicated that PTP1B plays as a negative regulator in both insulin and leptin signal pathways. PTP1B down-regulates insulin signaling cascades via the tyrosine dephosphorylation of the insulin receptor or insulin receptor substrates 1 and 2, preventing their interactions with downstream signaling molecules. PTP1B also negatively regulates the leptin signaling pathway by dephosphorylating phosphorylated tyrosine kinase JAK2 [5]. In vivo studies have demonstrated an increase in insulin sensitivity, glycemic control, and resistance to a high fat diet in PTP1B-deficient mice [6]. Reduction of PTP1B level decreases the adipose tissue mass, plasma insulin, and blood glucose levels in diabetic animal models [7]. These biochemical and pharmacological evidences suggested that the inhibition of PTP1B could be an effective strategy in the treatment of obesity, diabetes, and cancer, and that the development of new and effective PTP1B inhibitors is important and necessary. In line with this, PTP1B inhibitory effects of the isolated compounds were evaluated herein.

Supplementary information The online version of this article (https://doi.org/10.1038/s41429-019-0187-7) contains supplementary material, which is available to authorized users.

✉ Hyuncheol Oh
hoh@wonkwang.ac.kr

[1] College of Pharmacy, Wonkwang University, Iksan 54538, Republic of Korea

[2] Institute of Marine Biochemistry, Vietnam Academy of Science and Technology (VAST), 18 Hoang Quoc Viet, Cau Giay, Hanoi, Vietnam

[3] Institute of Genome Research, Vietnam Academy of Science and Technology (VAST), 18 Hoang Quoc Viet, Cau Giay, Hanoi, Vietnam

[4] College of Medical and Life Sciences, Silla University, Busan 46958, Republic of Korea

The fungal strain SF-5497 was cultured on 45 Fernbach flasks of potato dextrose agar (PDA) media containing 3% NaCl at 25 °C for 14 days. The culture plates were extracted with EtOAc, and the resultant extract was concentrated in vacuo to provide a residue. The residue was subjected to multiple chromatographic steps, including reversed-phase C_{18} column chromatography, and semi-preparative HPLC, to yield compounds **1**–**5** (Fig. 1a).

Compound **1** was isolated as a colorless gum. Its molecular formula was established as $C_{26}H_{38}O_8$ based on the observation of a sodium adduct ion peak at *m/z* 501.2438 $[M + Na]^+$ in the HRESITOFMS, along with analysis of ^1H and ^{13}C NMR data, implying eight degrees of unsaturation. The ^1H NMR spectrum (Table 1) displayed signals for two olefinic protons [δ_H 5.37 and 4.84 (each s, H-1′a and H-1′b)], six tertiary methyl groups [δ_H 1.23 (s, H_3-12), δ_H 0.94 (s, H_3-13), δ_H 1.17 (s, H_3-14), δ_H 1.24 (s, H_3-15), δ_H 1.45 (s, H_3-9′), and δ_H 1.36 (H_3-10′)], and one methoxy group at δ_H 3.70 (s). The ^{13}C NMR and DEPT spectra (Table 1) indicated the presence of 26 carbon signals, including seven methyls, six methylenes, two methines, and 11 non-protonated carbons (including four carbonyl carbons). In addition, analysis of the ^{13}C NMR spectrum suggested the presence of signals corresponding to two ketone carbonyl carbons [δ_C 208.1 (C-4′) and δ_C 203.8 (C-6′)], one carboxylic methyl ester [δ_C 168.7 (C-8′) and δ_C 52.5 (8′-OCH_3)], an exocyclic double bond [δ_C 112.4 (C-1′) and δ_C 145.8 (C-2′)], two quaternary carbons [δ_C 50.9 (C-3′) and δ_C 72.7 (C-7′)], a quaternary carbinolic carbon (δ_C 80.1, C-5′), and two methyl groups [δ_C 22.1 (C-9′) and δ_C 15.0 (C-10′)], suggesting the presence of a 2-hydroxy-2-methyl-1,3-dioxo partial structure (D ring), bearing methyl ester functionality [8, 9]. The assignment of this partial structure was confirmed by the HMBC correlations from H_2-1′ to C-2′, C-3′, and C-7′; from H_3-9′ to C-2′, C-3′, and C-4′; from H_3-10′ to C-4′, C-5′, and C-6′; and from δ_H 3.70 to C-8′ (Fig. 1b). Further detailed analysis of the ^1H and ^{13}C NMR spectroscopic data of **1** and comparison with those of the reported meroterpenoid, preaustinoid A1 revealed that the structures of these two compounds are very similar, but the difference was clearly presented at the A ring of preaustinoid A1 [9]. The up-field shifted ^{13}C chemical shifts of two methylene groups [δ_C 33.6 (C-1) and δ_C 27.8 (C-2)] and a non-protonated carbon (δ_C 75.8, C-4), as well as the down-field shifted chemical shift of the carbonyl carbon (δ_C 178.4, C-3) suggested the presence of a 4-hydroxy-3,4-seco-3-oic acid structural moiety in **1**. The partial structure corresponding to a 4-hydroxy-3,4-seco-3-oic acid moiety in **1** was assigned with the aid of HMBC correlations from H_3-14 and H_3-15 to C-4 and C-5; from H_2-1 to C-2 and C-3; and from H_2-2 to C-3, along with the COSY correlation between H_2-1 and H_2-2. This was further confirmed by a conversion of **1** to methyl ester **1a**. Upon methylation reaction in the presence of MeOH and trimethylsilyldiazomethane ($TMSCHN_2$), and followed by preparative TLC, compound **1** was converted to a methylated product **1a**, which was recently isolated from *Penicillim* sp. [10] and *Eupenicillium* sp. [11]. The relative configuration of **1** was determined by NOESY spectrum as well as the computer-generated lower energy conformation using MM2 force field calculations (Fig. 1c). In the NOESY spectrum, H-5 showed NOE correlation with H-9, indicating that H-5 and H-9 are both β-oriented. NOE correlations between H_3-13/H-11a and H_3-12; between H_3-12/H-11a and H_3-9′; and between H_3-9′/H-11a revealed that H_3-12, H_3-13, H_3-9′, and H-11a are α-oriented. Furthermore, NOE correlations observed between H-5/H-11b and H_3-10′ indicated the β-orientation of H_3-10′. Thus, the structure of **1** was established as shown in Fig. 1a, and was given the trivial name preaustinoid A6. The numbering system shown in **1** was chosen by analogy to that used in the literature for preaustinoids [8, 9].

Compound **2** was isolated as a colorless gum. Its molecular formula was determined to be $C_{26}H_{36}O_7$ (nine degrees of unsaturation) based on the observation of an ion peak at *m/z* 483.2356 $[M + Na]^+$ in the HRESITOFMS data. The ^1H NMR data (Table 1) showed signals for four olefinic protons [δ_H 5.28, δ_H 4.76 (each s, H-1′a, H-1′b); δ_H 4.84 and δ_H 4.64 (each s, H-14a and H-14b)], five tertiary methyl groups [δ_H 1.30 (s, H_3-12), δ_H 0.81 (s, H_3-13), δ_H 1.70 (s, H_3-15), δ_H 1.44 (s, H_3-9′), and δ_H 1.34 (s, H_3-10′)], and one methoxy group at δ_H 3.63 (s). Analysis of ^{13}C NMR, DEPT, and HMQC ($J_{CH} = 8$ Hz) correlations (Table 1) displayed the presence of 26 carbon signals, including six methyls, seven methylens, two methines, and 11 non-protonated carbons (including four carbonyl carbons). These data for **2** were similar to those of **1** except for the presence of signals corresponding to the terminal olefinic group [δ_C 148.0 (C-4) and δ_C 114.6 (C-14)], and the absence of a methyl group and one oxygenated carbon. The position of the terminal olefinic group was confirmed by ^1H–^{13}C long-range correlations of H-14a and H-14b with C-4, C-5, and C-15; H-15 with C-4 and C-14 (Fig. 1b). All the other key ^1H–^{13}C long-range correlations for **2** (Fig. 1b) enabled to assign the complete structure of this compound as shown in Fig. 1a, and named preaustinoid A7. The relative configuration of **2** was deduced by NOESY spectroscopic analysis. As with the case of **1**, the relative configuration of **2** was determined on the basis of the NOESY data. NOE correlations between H-5/H-9 and H-9/H_3-10′ suggested that these groups are on the β-oriented. On the other hand, NOE correlations of H_3-12 with H_3-13, H_3-9′, and H-14; of H_3-13 with H-14 and H_3-9′; and of H-1′a with H_3-9′ suggested that these groups are on the α-oriented. Thus, the relative configuration of **2** was suggested as shown in Fig. 1a.

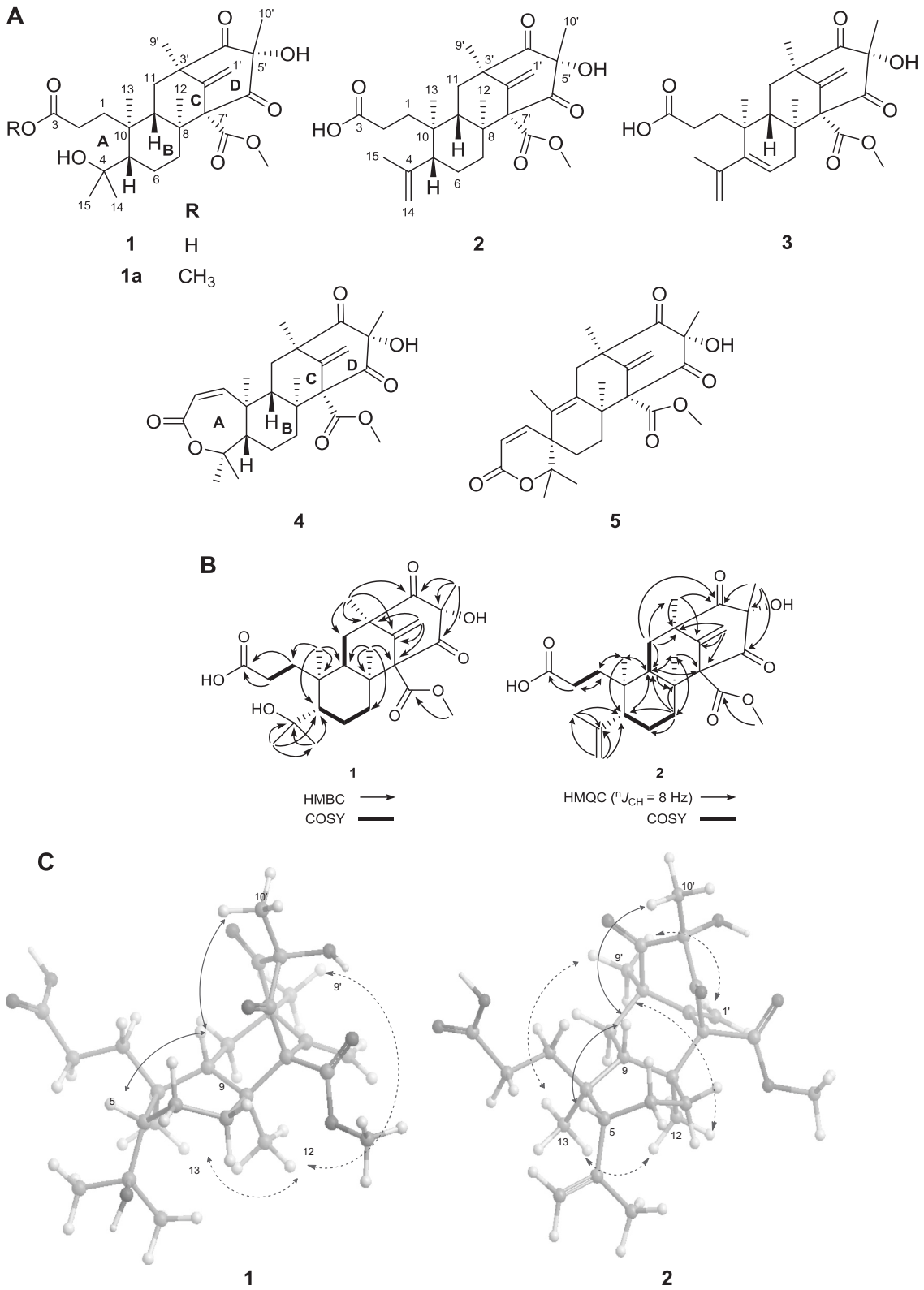

Fig. 1 **a** Chemical structures of compounds **1**–**5**. **b** Key HMBC or HMQC ($J_{CH} = 8$ Hz) and COSY correlations of compounds **1** and **2**. **c** Key NOESY correlations of compounds **1** and **2**

Table 1 ^{1}H and ^{13}C NMR data for preaustinoid A6 (**1**) and preaustinoid A7 (**2**)

Position	Preaustinoid A6 (1)		Preaustinoid A7 (2)	
	δ_C[a,b], type	δ_H[a,c] (*J* in Hz)	δ_C[b,d], type	δ_H[c,d] (*J* in Hz)
1	33.6, CH_2	2.43, m	35.3, CH_2	1.45, m
		1.54, m		1.45, m
2	27.8, CH_2	2.11, m	28.8, CH_2	1.99, m
		1.73, m		1.64, m
3	178.4, C		178.1, C[e]	
4	75.8, C		148.0, C	
5	50.8, CH	1.17, m	51.0, C	1.82, m
6	22.5, CH_2	2.41, m	25.7, CH_2	1.84, m
		1.53, m		1.38, m
7	32.4, CH_2	2.14, m	33.2, CH_2	2.11, m
		1.87, m		1.86, m
8	47.8, C		48.5, C[e]	
9	44.6, CH	0.62, dd (2.0, 13.6)	45.1, C	0.66, dd (2.9, 13.7)
10	42.1, C		41.0, C	
11	39.0, CH_2	1.96, dd (2.4, 13.2)	40.9, CH_2	1.84, m
		1.54, m		1.67, m
12	17.1, CH_3	1.23, s	17.7, CH_3	1.30, s
13	20.1, CH_3	0.94, s	20.5, CH_3	0.81, s
14	27.1, CH_3	1.17, s	114.6, CH_2	4.84, s
				4.64, s
15	34.3, CH_3	1.24, s	23.8, CH_3	1.70, s
1′	112.4, CH_2	5.37, s	111.9, CH_2	5.28, s
		4.84, s		4.76, s
2′	145.8, C		146.3, C	
3′	50.9, C		51.9, C	
4′	208.1, C		210.9, C	
5′	80.1, C		79.8, C	
6′	203.8, C		206.1, C	
7′	72.7, C		73.9, C	
8′	168.7, C		170.9, C	
9′	22.1, CH_3	1.45, s	22.3, CH_3	1.44, s
10′	15.0, CH_3	1.36, s	16.4, CH_3	1.34, s
8′-OCH_3	52.5, CH_3	3.70, s	52.2, CH_3	3.63, s

[a]Recorded in $CDCl_3$

[b]100 MHZ

[c]400 MHz

[d]Recorded in CD_3OD

[e]Not observed in the ^{13}C NMR, and assigned by analysis of HMQC ($J_{CH} = 8$ Hz) data

The structures of three known compounds were identified as berkeleyone C (**3**) [12], preaustinoid A2 (**4**) [9], and preaustinoid A3 (**5**) [13] by analyses of NMR and MS, along with comparisons of these data with those reported in the literature (Fig. 1a). The absolute configurations of **1a**, **3**, and **5** have been determined by ECD spectrum [11]. Since we observed negative specific rotations for **1a** and **3**, and positive-specific rotations for **5**, consistent with those in the literature, it was suggested that compounds **1a**, **3**, and **5** have the same absolute configurations as those defined in the literature [11]. In addition, the absolute configuration of compounds **1** and **2** were proposed to be analogous to those for **1a**, **3**, and **5** because they were produced by the same fungal strain.

As evidenced by many biochemical, genetic, and pharmacological studies, inhibition of PTP1B could be helpful in the treatment of human disorders, such as diabetes, obesity, and cancer [14]. To date, more than 300 PTP1B inhibitors have been discovered and developed from natural resources, of which two groups of phenolics and terpenoids have emerged as potential PTP1B inhibitors [15]. Although many natural PTP1B inhibitors exhibited promising clinical potential, there are no clinically used PTP1B inhibitors, which is most likely due to relatively low activities or lack of selectivity. Thus, searching for more potent and selective PTP1B inhibitors is still necessary. In the present study, the isolated compounds were evaluated for their inhibitory effects on PTP1B activity, and the result showed that compounds **1** and **3** inhibited PTP1B activity in a dose dependent manner, with IC_{50} values of 17.6 and 58.4 μM, respectively, while compounds **1a**, **2**, **4**, and **5** exhibited no inhibitory activity up to 100 μM. It is interesting to note that the conversion of acid functionality to methyl ester or minor structural modification at the A part of the compound **1** led to the significant reduction in PTP1B inhibitory activity.

To identify the PTP1B inhibitory characteristic of the active compound **1**, kinetic analysis was conducted using different concentrations of the compounds and *p*-NPP. The initial rate was determined on the basis of the rate of increase in absorbance at 405 nm. The Michaelis–Menten constant (K_m) and maximal velocity (V_{max}) of PTP1B were determined by Lineweaver–Burk plot analysis for competitive inhibition and the intercept on the vertical axis for noncompetitive inhibition (GraphPad Prism 5.01). As shown in Fig. 2, compound **1** lowered the apparent value of V_{max} and increased the K_m value, indicating that **1** inhibited PTP1B in a noncompetitive manner, with the K_i value of 17.0 μM. In addition, the plot in Fig. 2 displayed the lines converged to the left of the 1/[V] axis and above the 1/[S] axis ($\alpha > 1$). This observation suggested that compound **1** preferentially bound to the free enzyme than to the enzyme–substrate complex [16]. It is noted that the discovery of noncompetitive PTP1B inhibitors targeting the active site or allosteric of the enzyme could be potentially developed into effective and bioavailable PTP1B inhibitors, which are most challenging features of PTP1B inhibition-based drugs [17, 18]. Previously, berkeleyone C (**3**) was reported to possess inhibitory effect against the production

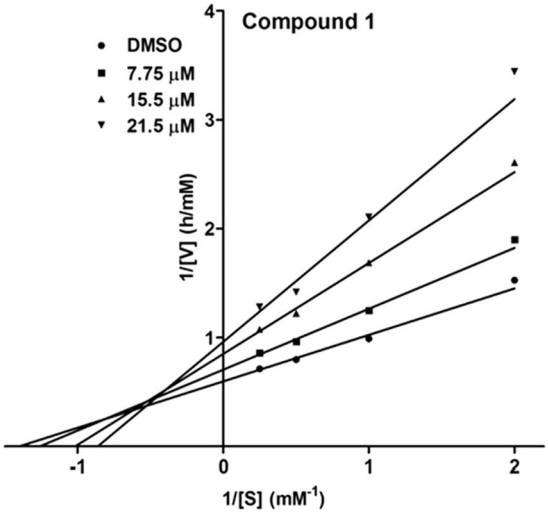

Fig. 2 Lineweaver–Burk plots for inhibition of PTP1B-catalyzed hydrolysis of *p*-NPP by compound **1**. Data are expressed as mean initial velocity for triplicate experiments ($n = 3$) at each substrate concentration

of interleukin-1β from induced inflammasomes in THP-1 cell line [12]. Although the PTP1B inhibitory effects of several meroterpenoids have been reported [19], to the best of our knowledge, this is the first case reporting the PTP1B inhibitory effects of the preaustinoid-related meroterpene derivatives. Further studies to assess the selectivity, bioavailability, and efficacy of these compounds are necessary to evaluate their potential as lead compounds in the treatment of diabetes and obesity based on the inhibition of PTP1B activity.

Acknowledgements This research was supported by Wonkwang University in 2018.

Compliance with ethical standards

Conflict of interest The authors declare that they have no conflict of interest.

Publisher's note: Springer Nature remains neutral with regard to jurisdictional claims in published maps and institutional affiliations.

References

1. Matsuda Y, Abe I. Biosynthesis of fungal meroterpenoids. Nat Prod Rep. 2016;33:26–53.
2. Kim D-C, et al. Dihydroisocoumarin derivatives from marine-derived fungal isolates and their anti-inflammatory effects in lipopolysaccharide-induced BV2 microglia. J Nat Prod. 2015; 78:2948–55.
3. Park JS, et al. Furanoaustinol and 7-acetoxydehydroaustinol: new meroterpenoids from a marine-derived fungal strain *Penicillium* sp. SF-5497. J Antibiot. 2018;71:557–63.
4. Combs AP. Recent advances in the discovery of competitive protein tyrosine phosphatase 1B inhibitors for the treatment of diabetes, obesity, and cancer. J Med Chem. 2010;53:2333–44.
5. Bence KK, et al. Neuronal PTP1B regulates body weight, adiposity and leptin action. Nat Med. 2006;12:917–24.
6. Payette P, et al. Increased insulin sensitivity and obesity resistance in mice lacking the protein tyrosine phosphatase-1B gene. Science. 1999;283:1544–8.
7. Zinker BA, et al. PTP1B antisense oligonucleotide lowers PTP1B protein, normalizes blood glucose, and improves insulin sensitivity in diabetic mice. Proc Natl Acad Sci USA. 2002; 99:11357–62.
8. dos Santos RMG, Rodrigues-Fo E. Meroterpenes from *Penicillium* sp. found in association with *Melia azedarach*. Phytochemistry. 2002;61:907–12.
9. dos Santos RMG, Rodrigues-Fo E. Further meroterpenes produced by *Penicillium* sp., an endophyte obtained from *Melia azedarach*. Z Naturforsch C. 2003;58c:663–9.
10. Duan R, et al. Antimicrobial meroterpenoids from the endophytic fungus *Penicillium* sp. T2-8 associated with *Gastrodia elata*. Phytochem Lett. 2016;18:197–201.
11. Gu B-B, et al. 3,5-Dimethylorsellinic acid derived meroterpenoids from *Eupenicillium* sp. 6A-9, a fungus isolated from the marine sponge *Plakortis simplex*. Eur J Org Chem. 2018;2018:48–59.
12. Stierle DB, et al. Berkeleyones and related meroterpenes from a deep water acid mine waste fungus that inhibit the production of interleukin 1-β from induced inflammasomes. J Nat Prod. 2011;74:2273–7.
13. Fill TP, Pereira GK, dos Santos RMG, Rodrigues-Fo E. Four additional meroterpenes produced by *Penicillium* sp. found in association with *Melia azedarach*. Possible biosynthetic intermediates to Austin. Z Naturforsch. 2007;62b:1035–44.
14. Zhang S, Zhang Z-Y. PTP1B as a drug target: recent developments in PTP1B inhibitor discovery. Drug Discov Today. 2007;12:373–81.
15. Jiang C-S, Liang LF, Guo Y-W. Natural products possessing protein tyrosine phosphatase 1B (PTP1B) inhibitory activity found in the last decades. Acta Pharmacol Sin. 2012;33:1217–45.
16. Copeland RA. Evaluation of enzyme inhibitors in drug discovery. New Jersey: John Wiley & Sons, Inc.; 2005. p. 48–81.
17. Wiesmann C, et al. Allosteric inhibition of protein tyrosine phosphatase 1B. Nat Struct Mol Biol. 2004;11:730–7.
18. Liu S, et al. Targeting inactive enzyme conformation: Aryl diketoacid derivatives as a new class of PTP1B inhibitors. J Am Chem Soc. 2008;130:17075–84.
19. Menna M, Imperatore C, D'Aniello F, Aiello A. Meroterpenes from marine invertebrates: structures, occurrence, and ecological implications. Mar Drugs. 2013;11:1602–43.